PLOS ONE

RESEARCH ARTICLE

Novel pathway for mutagenic tautomerization of classical A·T DNA base pairs *via* sequential proton transfer through quasi-orthogonal transition states: A QM/QTAIM investigation

Ol'ha O. Brovarets'[1,2], Kostiantyn S. Tsiupa[1], Dmytro M. Hovorun[1,2]*

1 Department of Molecular and Quantum Biophysics, Institute of Molecular Biology and Genetics, National Academy of Sciences of Ukraine, Kyiv, Ukraine, **2** Department of Molecular Biotechnology and Bioinformatics, Institute of High Technologies, Taras Shevchenko National University of Kyiv, Kyiv, Ukraine

* dhovorun@imbg.org.ua

Citation: Brovarets' OO, Tsiupa KS, Hovorun DM (2018) Novel pathway for mutagenic tautomerization of classical A·T DNA base pairs *via* sequential proton transfer through quasi-orthogonal transition states: A QM/QTAIM investigation. PLoS ONE 13(6): e0199044. https://doi.org/10.1371/journal.pone.0199044

Editor: Dennis Salahub, University of Calgary, CANADA

Received: February 11, 2018

Accepted: May 30, 2018

Published: June 27, 2018

Data Availability Statement: All relevant data are presented within the paper.

Funding: Brovarets' expresses sincere gratitude to organizing committee headed by Prof. Karl Kuchler (Medical University Vienna, Austria) for the financial support (ABC fellow) of her participation in the 7th FEBS Special Meeting "ATP-Binding Cassette (ABC) Proteins: From Multidrug Resistance to Genetic Disease" (March 6–12, 2018, Innsbruck, Austria) and to Chemistry

Abstract

In this paper we have theoretically predicted a novel pathway for the mutagenic tautomerization of the classical A·T DNA base pairs in the free state, the Watson-Crick A·T(WC), reverse Watson-Crick A·T(rWC), Hoogsteen A·T(H) and reverse Hoogsteen A·T(rH) pairs, *via* sequential proton transfer accompanied by a significant change in the mutual orientation of the bases. Quantum-mechanical (QM) calculations were performed at the MP2/aug-cc-pVDZ//B3LYP/6-311++G(d,p) level in vacuum phase, along with Bader's quantum theory of Atoms in Molecules (QTAIM). These processes involve transition states (TSs) with quasi-orthogonal structures (symmetry C_1), which are highly polar, tight ion pairs (A^-, $N6H_2$-deprotonated)·(T^+, O4/O2-protonated). Gibbs free energies of activation for the A·T(WC) / A·T(rWC) ↔ A*·T(rw_{WC}) / A*·T(w_{WC}) tautomeric transitions (~43.5 kcal·mol^{-1}) are lower than for the A·T(H) / A·T(rH) ↔ A^*_{N7}·T(rw_H) / A^*_{N7}·T(w_H) tautomerisations (~53.0 kcal·mol^{-1}) (rare tautomers are marked by an asterisk; w—wobble configured tautomerisation products). The (T)N3$^+$H···N1$^-$(A), (T)O4$^+$H···N1$^-$(A) / (T)N3$^+$H···N1$^-$(A) and (T)O2$^+$H···N1$^-$(A) H-bonds are found in the transition states $TS^{A^{-}\cdot T^{+}}_{A\cdot T(WC)\leftrightarrow A^{*}\cdot T(rwWC)}$ / $TS^{A^{-}\cdot T^{+}}_{A\cdot T(rWC)\leftrightarrow A^{*}\cdot T(wWC)}$. However, in the transition state $TS^{A^{-}\cdot T^{+}}_{A\cdot T(H)\leftrightarrow A^{*}N7\cdot T(rwH)}$ / $TS^{A^{-}\cdot T^{+}}_{A\cdot T(rH)\leftrightarrow A^{*}N7\cdot T(wH)}$, the (T)N3$^+$H···N7$^-$(A), (T)O4$^+$H···N7$^-$(A) / (T)N3$^+$H···N7$^-$(A) and (T)O2$^+$H···N7$^-$(A) H-bonds are supplemented by the attractive (T)O4$^+$/O2$^+$···N6$^-$(A) van der Waals contacts. It was demonstrated that the products of the tautomerization of the classical A·T DNA base pairs—A*·T(rw_{WC}), A^*_{N7}·T(rw_H) and A^*_{N7}·T(w_H) (symmetry C_s)–further transform *via* double proton transfer into the energetically favorable wobble A·T*(rw_{WC}), A·T*(rw_H) and A·T^*_{O2}(w_H) base mispairs (symmetry C_s).

Biological Interface Division of the Royal Society of Chemistry (RSC, UK) for the RSC Travel Grant for the participation at the "3rd Green and Sustainable Chemistry Conference" (May 13-16, 2018, Hotel Intercontinental, Berlin, Germany). The funders had no role in study design, data collection and analysis, decision to publish, or preparation of the manuscript.

Competing interests: The authors have declared that no competing interests exist.

Introduction

Investigation of microstructural mechanisms for mutagenic tautomerization of the Watson-Crick DNA base pairs occupies an important place in molecular biophysics and molecular biology, enabling an understanding of the nature of genome instability [1–5]. This follows from the 'rare tautomer hypothesis' proposed by Watson and Crick [1] shortly after they established the spatial architecture of DNA [2]. However, achievements in this area remain rather modest despite its long history [6], encouraging further research in this direction.

Löwdin [3, 4] first proposed that the electronic structure of the Watson-Crick (WC) DNA base pairs A·T(WC) and G·C(WC) permits their transition into the high-energy tautomerized states $A^*{\cdot}T^*$(L) and $G^*{\cdot}C^*$(L), now called Löwdin (L) base pairs. Here and henceforth, rare (in particular mutagenic) tautomers are marked with an asterisk and differ from each other by the location of a particular proton: in the A^* rare tautomer proton bonds to N1 nitrogen atom, A^*_{N7} –to N7 nitrogen atom; T^*–to O4 oxygen atom and T^*_{O2} –to O2 oxygen atom. Löwdin proposed that the A·T(WC)↔$A^*{\cdot}T^*$(L) and G·C(WC)↔$G^*{\cdot}C^*$(L) transitions occur by double proton transfer (DPT) along neighboring intermolecular hydrogen (H) bonds *via* proton tunneling. These ideas have been prominent in the field of quantum biology and attracted much theoretical study of the mechanisms of spontaneous transitions and transversions arising during DNA replication [7–14].

Recently, it has become clear that Löwdin's mechanism does not provide the generation of sufficiently long-lived mutagenic tautomers of the DNA bases, which escape from the replicative DNA-polymerase transforming into their canonical tautomeric forms. The root cause of this observation is the absence of the reverse barrier of tautomerization ΔΔG in the A·T(WC) DNA base pair and its small value in comparison with kT (0.62 kcal·mol^{-1} under normal conditions) for the G·C(WC) DNA base pair [8, 9, 15–18].

In previous papers [19–27] we proposed an alternative mechanism for mutagenic tautomerization of the A·T(WC) and G·C(WC) base pairs into the corresponding wobble base mispairs and *vice versa*, which mechanism obviates the above difficulties. The chief difference of our mechanism from the Löwdin mechanism is that, in the process of mutagenic tautomerization through sequential proton transfer, the DNA bases shift laterally relative each other into the DNA minor or major grooves, leading to the wobble configuration which contains the mutagenic tautomers [19]. Moreover, it turned out that a similar mechanism works also for the mutagenic tautomerization of purine-purine [21], pyrimidine-pyrimidine [22, 23] and purine-pyrimidine [24–27] DNA base mispairs, which are active players in the field of spontaneous point mutagenesis.

This allows us to assume that it is the intrapair tautomeric transition of the wobble pairs from the main tautomeric form into the rare one with a WC configuration or close to it, and *vice versa*, which is the key to understanding the microstructural mechanisms for spontaneous transitions and transversions during DNA biosynthesis [19–27]. Theoretical analyses of such mechanisms have been experimentally confirmed in part for the A·C(w) and G·T(w) purine-pyrimidine pairs [28–31].

This paper uses QM/QTAIM methods to explore new pathways for mutagenic tautomerization of the classical Watson-Crick A·T(WC), reverse Watson-Crick A·T(rWC), Hoogsteen A·T(H) and reverse Hoogsteen A·T(rH) base pairs with a remarkable biological meaning (for more details, see Refs. [32–49]). These are controlled by transition states with a quasi-orthogonal structure (symmetry C_1) which are highly polar tight ion pairs (A^-, $N6H_2$–deprotonated)·(T^+, O4/O2-deprotonated).

Computational methods

The geometries of all the investigated DNA base pairs and transition states (TSs) were optimized using the Gaussian'09 package [50]. The B3LYP/6-311++G(d,p) level of theory [51–55] was used. This level of theory has successfully proved itself for calculations of similar systems [56–63]. The study included harmonic frequency calculations (using a scaling factor of 0.9668 [64–66]) and intrinsic reaction coordinate (IRC) analysis in the forward and reverse directions from each TS using a Hessian-based predictor-corrector integration algorithm [67] at the B3LYP/6-311++G(d,p) level of theory successfully applied in the previous studies [16, 17, 68, 69]. Local minima and TSs (localized by the synchronous transit-guided quasi-Newton method [70]) were confirmed as such by the absence or presence, respectively, of one imaginary frequency. Standard TS theory was applied to estimate the activation barriers for the tautomerisation reactions [71]. Single point electronic energy calculations were performed for the B3LYP geometries at the MP2/aug-cc-pVDZ level of theory [72, 73]. MP2 has been successfully applied to gain chemical information about similar proton transfer reactions in DNA systems [74–79]. The choice of the MP2 level of theory is caused by the insignificant errors in comparison with CCSD(T) method, that was convincingly shown in the benchmark works of Hobza and Šponer [80, 81].

We have performed investigations for the isolated H-bonded pairs of nucleotide bases, that adequately reflects the processes occurring in real duplex environment [14, 30, 31]. At this we relied on experience received in the previous works [82–85] devoted to related topics and systems, where the negligibly small impact of the stacking and sugar-phosphate backbone on the tautomerisation processes has been shown.

The Gibbs free energy G for all structures was obtained in the following way:

$$G = Eel + Ecorr \tag{1}$$

where E_{el} = electronic energy, while E_{corr} = thermal correction to Gibbs free energy.

Electronic interaction energies ΔE_{int} were calculated at the MP2/6-311++G(2df,pd) level of theory as the difference between the total energy of the base pair and energies of the monomers and corrected for the basis set superposition error (BSSE) [86,87] through the counterpoise procedure [88,89] without consideration of the deformation energies of the monomers due to their relatively small values [90].

Bader's quantum theory of Atoms in Molecules (QTAIM) [91–96] was applied to analyse the electron density distribution, using the AIMAll package [97] for the wave functions obtained at the B3LYP/6-311++G(d,p) level of theory. Presence of a bond critical point (BCP), namely, the so-called (3,-1) BCP, and a bond path between non-covalently connected atoms, as well as a positive value of the Laplacian at this BCP ($\Delta\rho>0$), were considered as criteria for formation of an H-bond or attractive van der Waals contact [98–100].

The energies of the attractive van der Waals contacts [101, 102] in TSs for tautomeric transitions of the base pairs were calculated by the empirical Espinosa-Molins-Lecomte (EML) formula [103, 104] based on the electron density distribution at the (3,-1) BCPs of the specific contacts:

$$E = 0.5\mathrm{V(r)} \tag{2}$$

where V(r) = value of a local potential energy at the (3,-1) BCP.

Energies of conventional AH···B H-bonds were evaluated by the empirical Iogansen formula [105]:

$$E_{AH\cdots B} = 0.33 \cdot \sqrt{\Delta v - 40}, \tag{3}$$

where Δν = magnitude of the stretching frequency shift for the AH H-bonded group involved in the AH···B H-bond relative to the unbound group. Partial deuteration was applied in order to avoid the effect of vibrational resonances [106–114].

The atom numbering scheme for the DNA bases is as per convention [108].

Results and discussion

These novel pathways for the mutagenic tautomerization of four biologically important A·T DNA base pairs—Watson-Crick A·T(WC), reverse Watson-Crick A·T(rWC), Hoogsteen A·T (H) and reverse Hoogsteen A·T(rH) [32–49]–are portrayed in Figs 1 and 2, with data entered into Tables 1–3.

Conformers of the A·T base pairs remain plane symmetric structures along the entire IRC of tautomerization. This also holds for base pairs tautomerising *via* proton transfer along intermolecular H-bonds as per currently known mechanisms for mutagenic tautomerization of WC pairs [16, 17, 19, 49].

The A·T(WC) / A·T(rWC) / A·T(H) / A·T(rH) ↔ A^{*}·T(rw_{WC}) / A^{*}·T(w_{WC}) / $A^{*}{}_{N7}$·T(rw_{H}) / $A^{*}{}_{N7}$·T(w_{H}) tautomerisation reactions occur *via* the initial migration of proton localized at the N6 atom of the $N6H_2$ amino group, leading to the formation of the A^{+}·T^{-} ion pair and significant change of the mutual orientation of the bases within the pair, i.e. mutual transformation of the *cys* / *trans*↔*trans* / *cys*-orientation of the N1H and N9H bonds relative to each other (Fig 1). Our new mechanism is controlled by the TSs having quasi-orthogonal structures (symmetry C_1). Further proton transfers to the N1/N7 nitrogen atom causing the rotation of the base and formation of the terminal wobble base mispair. Each of these tautomeric conversions is followed by the asynchronous DPT along the intermolecular H-bonds in the wobble base mispairs (Fig 2).

In all four cases of the novel A·T(WC) / A·T(rWC) / A·T(H) / A·T(rH) ↔ A^{*}·T(rw_{WC}) / A^{*}·T(w_{WC}) / $A^{*}{}_{N7}$·T(rw_{H}) / $A^{*}{}_{N7}$·T(w_{H}) tautomerisation reactions, the TSs are highly polar (~ 6.8–12.7 D) tight ion pairs (energy of interaction between bases in the pairs ~117–142 kcal·mol^{-1}) (Table 2). These TSs are (A^{-}, $N6H_2$-deprotonated)·(T^{+}, O4/O2-protonated) ion pairs. In the $TS^{A^{-}\cdot T^{+}}{}_{A\cdot T(WC)\leftrightarrow A^{*}\cdot T(rwWC)}$ / $TS^{A^{-}\cdot T^{+}}{}_{A\cdot T(rWC)\leftrightarrow A^{*}\cdot T(wWC)}$ transition states of tautomerisation the (T)$N3^{+}H\cdots N1^{-}$(A) (13.06 / 13.24) and (T)$O4^{+}$ / $O2^{+}H\cdots N1^{-}$(A) (8.85 / 8.82 kcal·mol^{-1}) are observed, while for the $TS^{A^{-}\cdot T^{+}}{}_{A\cdot T(H)\leftrightarrow A^{*}N7\cdot T(rwH)}$ / $TS^{A^{-}\cdot T^{+}}{}_{A\cdot T(rH)\leftrightarrow A^{*}N7\cdot T(wH)}$ transition states, the (T)$N3^{+}H\cdots N7^{-}$(A) (8.98 / 8.46) and (T)$O4^{+}$ / $O2^{+}H\cdots N7^{-}$(A) (5.18 / 4.38) H-bonds are supplemented by attractive (T)$O4^{+}$/$O2^{+}\cdots N6^{-}$(A) (2.58 / 3.71 kcal·mol^{-1}) van der Waals contacts (Fig 1, Table 2). At this, the (T)$N3^{+}H\cdots N1^{-}$/$N7^{-}$(A) H-bonds (~ 8.5–13.0 kcal·mol^{-1}) are significantly stronger than other specific contacts with increased ellipticity. The weakest among them are the attractive (T)$O4^{+}$/$O2^{+}\cdots N6^{-}$(A) (2.58 / 3.71 kcal·mol^{-1}) van der Waals contacts (Table 2).

All $TS_{A^{*}\cdot T(rwWC)\leftrightarrow A\cdot T^{*}(rwWC)}$, $TS_{A^{*}\cdot T(wWC)\leftrightarrow A\cdot T^{*}O2(wWC)}$, $TS_{A^{*}N7\cdot T(rwH)\leftrightarrow A\cdot T^{*}(rwH)}$ and $TS_{A^{*}N7\cdot T(wH)\leftrightarrow A\cdot T^{*}O2(wH)}$ of the DPT reactions are stabilized by the N6-H-N3 covalent bridge and one-single intermolecular H-bond—N1H···O4 (11.61), N1H···O2 (10.94), N7H···O4 (13.76) and N7H···O4 (12.95 kcal·mol^{-1}), accordingly (Fig 2, Table 2).

The non-canonical CH···O H-bonds [110, 111] have been registered in the initial complexes of the tautomerisation: A·T(WC)–C2H···O2 (0.74), $A^{*}\cdot T^{*}$(L)–C2H···O2 (0.57), A·T (rWC)–C2H···O4 (0.77), A·T(H)–C8H···O2 (0.83), A·T(rH)–C8H···O4 (0.86 kcal·mol^{-1}), which are characterized by low energies $E_{CH\cdots O}$, estimated by the Espinose-Molins-Lecomte formula [103, 104], decreased electron-topological parameters (ρ, Δρ, 100·ε) and angles (∠AH···B), but increased intermolecular distances ($d_{C\cdots O}$ and $d_{H\cdots O}$) in comparison with the canonical H-bonds (for more details see Table 2).

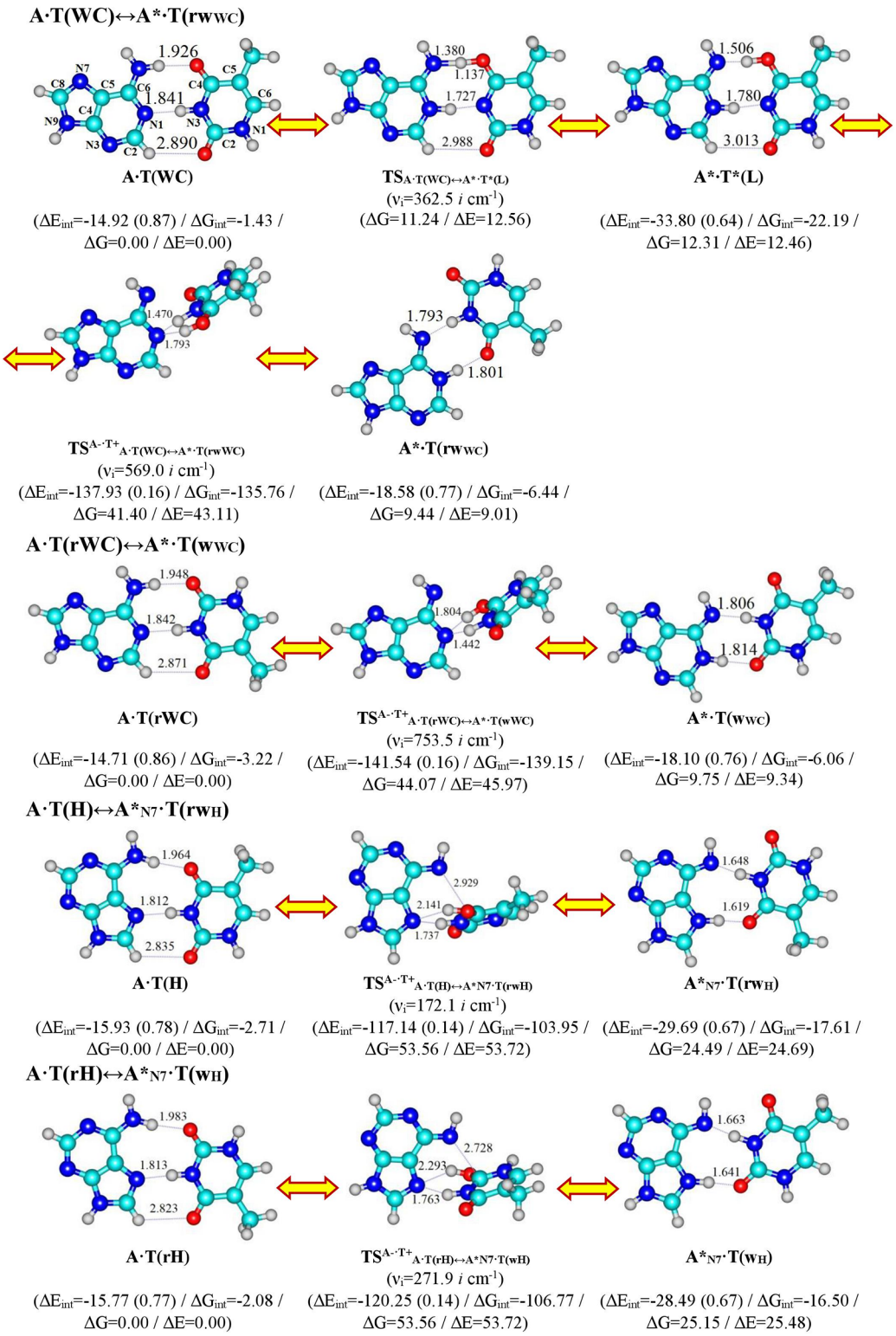

Fig 1. Geometrical structures of the stationary points on the discovered pathways of the tautomerizations *via* the sequential proton transfer in the four biologically important A·T DNA base pairs through the TSs with quasi-orthogonal oriented bases. Electronic ΔE_{int} (contribution of the total energy of the intermolecular specific contacts) and Gibbs free ΔG_{int} energies of the interaction (MP2/6-311++G(2df,pd)//B3LYP/6-311++G(d,p) level of theory, in kcal·mol^{-1}), relative Gibbs free energies ΔG and electronic energies ΔE (in kcal·mol^{-1}), imaginary frequencies ν_i at the TSs of the

conformational transitions (MP2/aug-cc-pVDZ//B3LYP/6-311++G(d,p) level of theory in the continuum with ε = 1 at T = 298.15 K) are presented below complexes in brackets. Dotted lines indicate AH···B H-bonds and attractive A···B van der Waals contacts—their lengths H···B and A···B are presented in angstroms (for their more detailed physico-chemical characteristics see Table 2); carbon atoms are in light-blue, nitrogen—in dark-blue, hydrogen—in grey and oxygen—in red.

https://doi.org/10.1371/journal.pone.0199044.g001

In general, the values of the electron density ρ at the (3,-1) BCPs of the intermolecular H-bonds range from 0.013 a.u. up to the 0.107 a.u.; the values of the Laplacian of the electron density Δρ at the (3,-1) BCPs are positive for all intrapair H-bonds and lie within a wide range from 0.005 a.u. up to the 0.152 a.u., demonstrating that H-bonds are attractive closed-shell ineractions; the value of the ellipticity ε varies in the range 0.79–8.6·10^{-3} (Table 2).

The classical geometrical criteria are satisfied for all canonical H-bonds in the investigated base mispairs and TSs of their interconversions: $d_{A\cdots B}$ (2.574–3.103 Å), $d_{H\cdots B}$ (1.442–2.293 Å) and ∠AH···B (139.2–179.3˚) (Table 2).

Interestingly, the energy of the intermolecular specific contacts (H-bonds and attractive van der Waals contacts) constitute only a minor part of the electronic energy of monomeric interactions for all these H-bonded structures (~14–0.87%) (see Figs 1 and 2). This agrees with previous results for other H-bonded base pairs [112].

All tautomeric transitions in this work are dipole-active, being accompanied by significant changes in dipole moment of the tautomerizing structures along the IRC (0.38–12.65 D), achieving maximum values for each tautomeric transition at its TS (7.38, 6.83, 12.65 and 10.636 D, accordingly) (Table 2). The Gibbs free energy of activation for the A·T(WC)/A·T(rWC)↔A^*·T(rw_{WC})/A^*·T(w_{WC}) tautomerisations (~ 43.5 kcal·mol^{-1}) is noticeably lower than for the A·T(H)/A·T(rH)↔A·T^*(rw_H)/A·T^*_{O2}(w_H) tautomerisations (~ 53.0 kcal·mol^{-1}) (Figs 1 and 2).

Note that only one case of mutagenic tautomerization, the A·T(WC)↔A^*·T(rw_{WC}) reaction, occurs by participation of the dynamically unstable intermediate A^*·T^*(L) (a Löwdin's base pair [3, 4]). The other three A·T DNA base pairs—A·T(rWC), A·T(H) and A·T(rH)–do not tautomerise *via* the Löwdin's mechanism. For these three pairs, the local minima corresponding to the tautomerized A^*·T^*_{O2}, A^*_{N7}·T^* and A^*_{N7}·T^*_{O2} base pairs are absent on the energy hypersurface. This observation is independent of the level of QM theory used.

It should be noted that three out of four tautomerization processes of the A·T base pairs do not complete with formation of the A^*·T(rw_{WC}), A^*_{N7}·T(rw_H) and A^*_{N7}·T(w_H) mispairs (Fig 2 and Table 1). These plane-symmetric wobble pairs (symmetry C_s) tautomerise further *via* the DPT mechanism along neighboring intermolecular H-bonds into the energetically-favorable plane-symmetric A·T^*(rw_{WC}), A·T^*(rw_H) and A·T^*_{O2}(w_H) DNA base mispairs, respectively (Fig 2, Tables 1 and 2). These processes occur *via* a concerted asynchronous mechanism with proton transfer along the intermolecular (T)N3H···N6(A) H-bonds, which, in fact, is a rate-limiting stage. It is noteworthy that the A^*_{N7}·T(rw_H)→A·T^*(rw_H) and A^*_{N7}·T(w_H)→A·T^*_{O2}(w_H) tautomerisations are barrier-less ($\Delta\Delta G_{TS}$ = -1.98 and -1.97 kcal·mol^{-1}) (Table 1), while the activation barriers for the A^*·T(rw_{WC})↔A·T^*(rw_{WC}) (1.39) and A^*·T(w_{WC})↔A·T^*_{O2}(w_{WC}) (1.77) are significantly lower than for the novel tautomerisation reactions (41.40–53.56 kcal·mol^{-1}), but are comparable with the values for the other DPT reactions [113]: from 2.42 for A^*·G^*_{syn}↔A·G^*_{syn} [100] to 10.29 kcal·mol^{-1} for A·T↔A^*·T^* [16] DPT tautomerisations.

It is thus possible to say that the tautomerization processes described here terminate with the mutagenic tautomerization of both T and A DNA bases with further formation of the classical mutagenic tautomers T^*, T^*_{O2} [16, 19, 27, 64, 102, 106] and A^* [16, 19–22, 25, 26, 100, 114], respectively. In this case, the A^*_{N7}·T(rw_H)↔A·T^*(rw_H) and A^*_{N7}·T(w_H)↔A·T^*_{O2}(w_H) tautomeric equilibria are completely shifted to the right. For the two other cases, the following

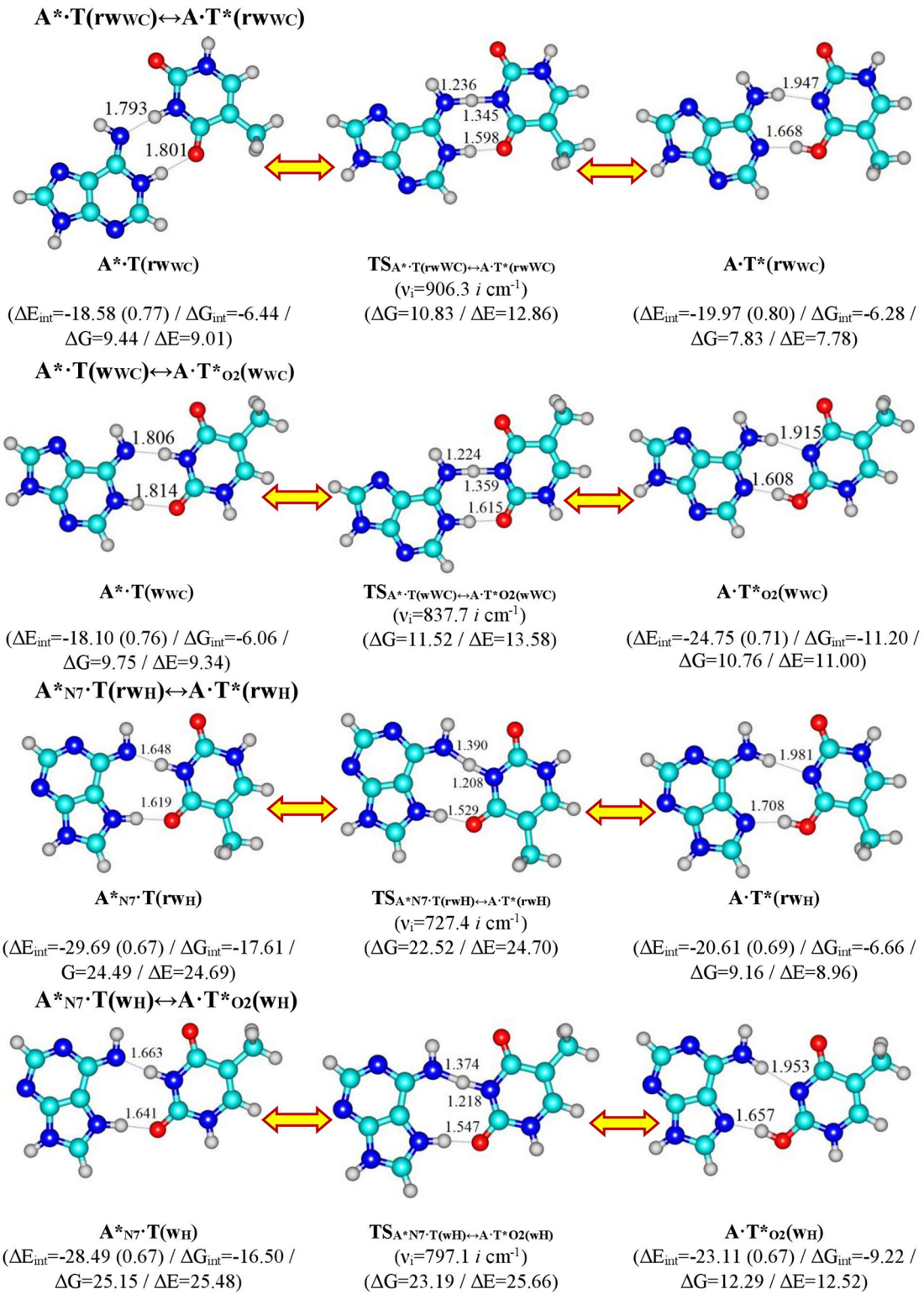

Fig 2. Geometrical structures of the stationary points on the pathways of the tautomerizations *via* the double proton transfer in the products of the discovered tautomerizations of the classical A·T DNA base pairs. For the detailed designations see Fig 1.

https://doi.org/10.1371/journal.pone.0199044.g002

Table 1. Energetic characteristics (in kcal·mol^{-1}) of the discovered mutagenic tautomerizations of the biologically important A·T DNA base pairs *via* the single and double proton transfers obtained at the MP2/aug-cc-pVDZ//B3LYP/6-311++G(d,p) level of QM theory in the continuum with ε = 1 under normal conditions (see Figs 1 and 2).

Tautomeric transition	ν_i[a]	ΔG[b]	ΔE[c]	$\Delta\Delta G_{TS}$[d]	$\Delta\Delta E_{TS}$[e]	$\Delta\Delta G$[f]	$\Delta\Delta E$[g]
A·T(WC)↔A*·T*(L)	362.5	12.31	12.46	11.24	12.56	-1.07	0.10
A*·T*(L)↔A*·T(rw_{WC})	569.0	9.44	9.01	41.40	43.11	31.95	34.10
A·T(rWC)↔A*·T(w_{WC})	753.5	9.75	9.34	44.07	45.97	34.32	36.63
A·T(H)↔A*$_{N7}$·T(rw_H)	172.1	24.49	24.69	52.59	52.49	28.10	27.80
A·T(rH)↔A*$_{N7}$·T(w_H)	271.9	25.15	25.48	53.56	53.72	28.41	28.24
A*·T(rw_{WC})↔A·T*(rw_{WC})	906.3	-1.61	-1.24	1.39	3.85	3.00	5.08
A*·T(w_{WC})↔A·T*$_{O2}$(w_{WC})	837.7	1.01	1.66	1.77	4.24	0.76	2.58
A*$_{N7}$·T(rw_H)↔A·T*(rw_H)	727.4	-15.34	-15.73	-1.98	0.01	13.36	15.73
A*$_{N7}$·T(w_H)↔A·T*$_{O2}$(w_H)	797.1	-12.87	-12.96	-1.97	0.18	10.90	13.14

[a]Imaginary frequency at the TS of the tautomeric transition, cm^{-1}.

[b]The Gibbs free energy of the product relatively the reactant of the tautomeric transition (T = 298.15 K).

[c]The electronic energy of the product relatively the reactant of the tautomeric transition.

[d]The Gibbs free energy barrier for the forward tautomeric transition.

[e]The electronic energy barrier for the forward tautomeric transition.

[f]The Gibbs free energy barrier for the reverse tautomeric transition.

[g]The electronic energy barrier for the reverse tautomeric transition.

https://doi.org/10.1371/journal.pone.0199044.t001

proportions are observed: A*·T(rw_{WC}) (6.9%) ↔ A·T*(rw_{WC}) (93.1%) and A*·T(w_{WC}) (83.6%) ↔ A·T*$_{O2}$(w_{WC}) (16.4%).

Gibbs free energies (in kcal·mol^{-1}) and populations of the investigated base mispairs yield the order: A·T(H) (0.00) < A·T(rH) (0.22/0.63) < A·T(WC) (1.05/0.21) < A·T(rWC) (1.31/0.16) < A·T*(rw_{WC}) (8.83/3.77·10^{-7}) < A·T*(rw_H) (8.96/1.92·10^{-7}) < A*·T(rw_{WC}) (10.07/2.47·10^{-8}) < A*·T(w_{WC}) (10.65/1.13·10^{-8}) < A·T*$_{O2}$(w_{WC}) (12.31/2.07·10^{-9}) < A·T*$_{O2}$(w_H) (12.74/6.13·10^{-10}) < A*·T*(L) (13.51/1.95·10^{-10}) < A*$_{N7}$·T(rw_H) (24.69/1.08·10^{-18}) < A*$_{N7}$·T(w_H) (25.70/2.24·10^{-19}). Notably, populations of the wobble A·T*(rw_{WC}), A·T*(rw_H), A*·T(rw_{WC}), A*·T(w_{WC}), A·T*$_{O2}$(w_{WC}), A·T*$_{O2}$(w_H) (12.74/6.13·10^{-10}) and A*·T*(L) tautomerised states, fitting into the range of the frequencies of the spontaneous point mutations observed experimentally (10^{-11}–10^{-9}) [115–117], point on their involvement into the processes of the origin of the spontaneous point mutations.

Notably, the methyl group of the T DNA base does not change its orientation during all these tautomerisation processes without exception. Moreover, the heterocycles of the DNA bases remain planar, despite their ability for out-of-plane bending [118–120].

A relatively small non-planarity of the pyrimidine ring of the protonated T$^+$ base occurs only in the $TS^{A\cdot\cdot T+}_{A\cdot T(WC)\leftrightarrow A^*\cdot T(rwWC)}$, $TS^{A\cdot\cdot T+}_{A\cdot T(rWC)\leftrightarrow A^*\cdot T(wWC)}$, $TS^{A\cdot\cdot T+}_{A\cdot T(H)\leftrightarrow A^*N7\cdot T(rwH)}$ and $TS^{A\cdot\cdot T+}_{A\cdot T(rH)\leftrightarrow A^*N7\cdot T(wH)}$ transition states. The maximum value of the non-planar dihedral angle reaches 2.5˚ (C2-N3-C4-C5), 3.1˚ (N1-C2-N3-C4), 3.7˚ (C2-N3-C4-C5) and 7.8˚ (N1-C2-N3-C4), respectively. Another structural feature of the protonated T$^+$ base in these TSs is the deviation of the O4$^+$H / O2$^+$H hydroxyl group from the plane of the pyrimidine ring (the dihedral angles range from 9.3 to 40.1˚) (Table 3).

Conclusions and perspectives

Novel pathways for mutagenic tautomerization of four classical A·T DNA base pairs, followed by the significant changes of base orientation within the pair, have been predicted by these QM results. The transition states with quasi-orthogonal structure (symmetry C_1) are highly polar

Table 2. Electron-topological, geometrical and energetic characteristics of the intermolecular specific contacts—H-bonds and attractive van der Waals (vdW) contacts in the investigated DNA base pairs and TSs of their tautomeric transformations obtained at the B3LYP/6-311++G(d,p) level of QM theory (ε = 1) (see Figs 1 and 2).

Complex	AH···B H-bond / A···B vdW contact	ρ^a	$\Delta\rho^b$	$100\cdot\varepsilon^c$	$d_{A\cdots B}{}^d$	$d_{H\cdots B}{}^e$	∠AH···B^f	$E_{AH\cdots B}$ $E_{A\cdots B}{}^g$	μ^h
A·T(WC) [16, 19]	N6H···O4	0.026	0.093	4.39	2.946	1.926	173.5	4.65	1.88
	N3H···N1	0.040	0.093	6.49	2.886	1.841	178.8	7.58	
	C2H···O2	0.004	0.014	3.40	3.975	2.890	132.3	0.74*	
$TS_{A\cdot T(WC)\leftrightarrow A^*\cdot T^*(L)}$	N1H···N3	0.052	0.101	6.08	2.775	1.727	171.4	9.62**	0.38
	C2H···O2	0.004	0.012	14.48	3.722	2.988	125.3	0.61*	
$A^*\cdot T^*$(L)	O4H···N6	0.087	0.065	4.56	2.578	1.506	174.8	13.47	0.78
	N1H···N3	0.045	0.101	6.24	2.825	1.780	171.1	7.73	
	C2H···O2	0.003	0.012	3.40	4.098	3.013	125.1	0.57*	
$TS^{A^{-}\cdot T^{+}}_{A\cdot T(WC)\leftrightarrow A^*\cdot T(rwWC)}$	$N3^+H\cdots N1^-$	0.100	0.026	5.89	2.583	1.470	158.1	13.06	7.38
	$O4^+H\cdots N1^-$	0.045	0.092	10.15	2.740	1.793	154.7	8.85	
$A^*\cdot T(rw_{WC})$	N3H···N6	0.044	0.095	6.22	2.844	1.793	174.7	8.53	3.23
	N1H···O4	0.035	0.117	3.55	2.832	1.801	177.3	5.82	
$TS_{A^*\cdot T(rwWC)\leftrightarrow A\cdot T^*(rwWC)}$	N1H···O4	0.061	0.142	3.32	2.663	1.598	179.3	11.61**	3.78
$A\cdot T^*(rw_{WC})$	N6H···N3	0.030	0.087	7.07	2.682	1.668	170.4	5.76	2.52
	O4H···N1	0.059	0.096	5.10	2.955	1.947	167.0	10.21	
A·T(rWC) [42]	N6H···O2	0.024	0.088	5.26	2.962	1.949	172.9	4.38	2.40
	N3H···N1	0.039	0.093	6.51	2.887	1.843	177.7	7.55	
	C2H···O4	0.004	0.014	3.32	3.696	2.872	132.8	0.77*	
$TS^{A^{-}\cdot T^{+}}_{A\cdot T(rWC)\leftrightarrow A^*\cdot T(wWC)}$	$N3^+H\cdots N1^-$	0.107	0.005	5.60	2.574	1.442	158.2	13.24	6.83
	$O2^+H\cdots N1^-$	0.043	0.090	9.82	2.741	1.804	152.8	8.82	
$A^*\cdot T(w_{WC})$	N3H···N6	0.042	0.095	6.21	2.858	1.806	173.3	8.31	4.29
	N1H···O2	0.034	0.115	4.40	2.845	1.814	177.0	5.49	
$TS_{A^*\cdot T(wWC)\leftrightarrow A\cdot T^*O2(wWC)}$	N1H···O2	0.058	0.141	4.10	2.676	1.615	179.2	10.94***	5.33
$A\cdot T^*_{O2}(w_{WC})$	N6H···N3	0.034	0.088	1.71	2.944	1.915	167.1	6.19	3.96
	O2H···N1	0.071	0.081	0.86	2.644	1.608	171.9	11.43	
A·T(H) [42]	N6H′···O4	0.023	0.086	3.93	2.972	1.963	170.6	4.18	6.16
	N3H···N7	0.041	0.099	5.75	2.853	1.811	175.9	7.39	
	C8H···O2	0.005	0.016	7.71	3.524	2.835	121.7	0.83*	
$TS^{A^{-}\cdot T^{+}}_{A\cdot T(H)\leftrightarrow A^*N7\cdot T(rwH)}$	$N3^+H\cdots N7^-$	0.050	0.097	4.51	2.754	1.737	158.7	8.98	12.65
	$O4^+H\cdots N7^-$	0.019	0.058	9.97	3.021	2.141	147.7	5.18	
	$O4^+\cdots N6^-$	0.013	0.043	68.81	2.929	-	-	2.58*	
$A^*_{N7}\cdot T(rw_H)$	N3H···N6	0.062	0.090	5.55	2.731	1.648	174.5	11.26	9.42
	N7H···O4	0.055	0.147	2.33	2.671	1.619	175.8	8.61	
$TS_{A^*N7\cdot T(rwH)\leftrightarrow A\cdot T^*(rwH)}$	N7H···O4	0.070	0.151	2.34	2.603	1.529	175.7	13.76**	8.37
$A\cdot T^*(rw_H)$	N6H′···N3	0.027	0.082	7.62	3.000	1.981	175.7	5.09	7.36
	O4H···N7	0.052	0.102	4.48	2.702	1.708	166.4	9.18	
A·T(rH) [42]	N6H′···O2	0.022	0.082	4.95	2.994	1.986	170.9	3.90	5.67
	N3H···N7	0.041	0.099	5.80	2.856	1.815	176.9	7.34	
	C8H···O4	0.005	0.017	7.97	3.517	2.825	121.9	0.86*	
$TS_{A\cdot T(rH)\leftrightarrow A^*N7\cdot T(wH)}$	$N3^+H\cdots N7^-$	0.047	0.098	3.26	2.757	1.763	154.8	8.46	10.36
	$O2^+H\cdots N7^-$	0.014	0.044	12.37	3.103	2.293	139.2	4.38	
	$O2^+\cdots N6^-$	0.018	0.055	78.70	2.829	-	-	3.71*	
$A^*_{N7}\cdot T(w_H)$	N3H···N6	0.060	0.092	5.58	2.743	1.663	175.7	10.97	10.35
	N7H···O2	0.051	0.145	3.17	2.689	1.641	176.3	8.09	
$TS_{A^*N7\cdot T(wH)\leftrightarrow A\cdot T^*O2(wH)}$	N7H···O4	0.067	0.152	3.15	2.615	1.547	176.3	12.95**	9.46

(*Continued*)

Table 2. (Continued)

Complex	AH···B H-bond / A···B vdW contact	ρ^a	$\Delta\rho^b$	$100\cdot\varepsilon^c$	$d_{A\cdots B}{}^d$	$d_{H\cdots B}{}^e$	∠AH···B^f	$E_{AH\cdots B}$ $E_{A\cdots B}{}^g$	μ^h
A·T*$_{O2}$(w$_H$)	N6H′···N3	0.029	0.086	7.38	2.974	1.953	176.4	5.38	8.23
	O2H···N7	0.059	0.100	4.48	2.664	1.657	168.0	10.16	

[a]The electron density at the (3,-1) BCP of the specific contact, a.u.

[b]The Laplacian of the electron density at the (3,-1) BCP of the specific contact, a.u.

[c]The ellipticity at the (3,-1) BCP of the specific contact.

[d]The distance between the A and B atoms of the of the AH···B / A···B specific contact, Å.

[e]The distance between the H and B atoms of the AH···B H-bond, Å.

[f]The H-bond angle, degree.

[g]Energy of the specific contact, calculated by Iogansen's [105], Espinose-Molins-Lecomte [103, 104] (marked with an asterisk) or Nikolaienko-Bulavin-Hovorun [109] (marked with double asterisk) formulas, kcal·mol^{-1}.

[h]The dipole moment of the complex, D.

https://doi.org/10.1371/journal.pone.0199044.t002

Table 3. Selected geometrical parameters, characterizing the non-planarity of the discovered mutagenic tautomerizations of the biologically important A·T DNA base pairs *via* the single and double proton transfers, obtained at the B3LYP/6-311++G(d,p) level of QM theory in the continuum with ε = 1.

TS of tautomerisation	Dihedral angles, degree	
	(A)N7C5(T)N3C4	(T)HO4/O2C4/C2N3
$TS^{A^{-}\cdot T^{+}}_{A\cdot T(WC)\leftrightarrow A^{*}\cdot T(rwWC)}$	85.0	-9.3
$TS^{A^{-}\cdot T^{+}}_{A\cdot T(rWC)\leftrightarrow A^{*}\cdot T(wWC)}$	60.4	11.8
$TS^{A^{-}\cdot T^{+}}_{A\cdot T(H)\leftrightarrow A^{*}N7\cdot T(rwH)}$	-99.0	-19.9
$TS^{A^{-}\cdot T^{+}}_{A\cdot T(rH)\leftrightarrow A^{*}N7\cdot T(wH)}$	-119.4	40.1

https://doi.org/10.1371/journal.pone.0199044.t003

tight ion pairs (A$^-$, N6H$_2$-deprotonated)·(T$^+$, O4/O2-protonated). The tautomerization products—the A*·T(rw$_{WC}$), A$^*_{N7}$·T(rw$_H$) and A$^*_{N7}$·T(w$_H$) pairs—further transform *via* concerted asynchronous double proton transfer into the energetically favorable wobble A·T*(rw$_{WC}$), A·T*(rw$_H$) and A·T$^*_{O2}$(w$_H$) mispairs (symmetry C$_s$), respectively. Moreover, it was established in our recent papers, that wobble A*·T(rw$_{WC}$) base mispair can also be formed from the reverse A·T(rWC) base pair [20], A*·T(wWC) base mispair—from the canonical A·T(rWC) base pair [19] and A$^*_{N7}$·T(w$_H$) base mispair—from the Hoogsteen A·T(H) base pair [20].

We are currently engaged in elaborating this topic in order to discover biologically important H-bonded nucleobase pairs, for which the mechanism of mutagenic tautomerization plays a key role. Moreover, we suggested that novel mechanism of mutagenic tautomerization presented in this study could lead to the conversion of an anti-parallel DNA helix to a parallel DNA helix. We also consider investigation of these tautomerisation mechanism by the participation of the modified A·T base pairs [121–124] as a task for the future.

Supporting information

S1 Dataset. Cartesian coordinates of the investigated complexes: A·T(WC); TS$_{A\cdot T(WC)\leftrightarrow A^*\cdot T^*(L)}$; A*·T*(L); TSA-·T+A·T(WC)↔A*·T(rwWC); A*·T(rw$_{WC}$); TS$_{A^*\cdot T(rwWC)\leftrightarrow A\cdot T^*(rwWC)}$; A·T*(rw$_{WC}$); A·T(rWC); TSA-·T+A·T(rWC)↔A*·T(wWC); A*·T(w$_{WC}$); TS$_{A^*\cdot T(wWC)\leftrightarrow A\cdot T^*O2(wWC)}$; A·T$^*_{O2}$(w$_{WC}$); A·T(H); TSA-·T+A·T(H)↔A*N7·T(rwH); A$^*_{N7}$·T(rw$_H$); TS$_{A^*N7\cdot T(rwH)\leftrightarrow A\cdot T^*(rwH)}$; A·T*(rw$_H$); A·T(rH); TS$_{A\cdot T(rH)\leftrightarrow A^*N7\cdot T(wH)}$; A$^*_{N7}$·T(w$_H$); TS$_{A^*N7\cdot T(wH)\leftrightarrow A\cdot T^*O2(wH)}$; A·T$^*_{O2}$(w$_H$).
(DOC)

Acknowledgments

The authors gratefully appreciate technical support and computational facilities of joint computer cluster of SSI "Institute for Single Crystals" of the National Academy of Sciences of Ukraine (NASU) and Institute for Scintillation Materials of the NASU incorporated into Ukrainian National Grid.

Author Contributions

Conceptualization: Dmytro M. Hovorun.

Data curation: Ol'ha O. Brovarets', Dmytro M. Hovorun.

Formal analysis: Ol'ha O. Brovarets', Kostiantyn S. Tsiupa, Dmytro M. Hovorun.

Funding acquisition: Dmytro M. Hovorun.

Investigation: Ol'ha O. Brovarets', Kostiantyn S. Tsiupa, Dmytro M. Hovorun.

Methodology: Kostiantyn S. Tsiupa, Dmytro M. Hovorun.

Project administration: Ol'ha O. Brovarets', Dmytro M. Hovorun.

Resources: Ol'ha O. Brovarets', Dmytro M. Hovorun.

Software: Dmytro M. Hovorun.

Supervision: Dmytro M. Hovorun.

Writing – original draft: Ol'ha O. Brovarets'.

Writing – review & editing: Ol'ha O. Brovarets', Kostiantyn S. Tsiupa, Dmytro M. Hovorun.

References

1. Watson JD, Crick FHC. The Structure of DNA. Cold Spring Harb Symp Quant Biol. 1953; 18: 123–131. PMID: 13168976
2. Watson JD, Crick FHC. Molecular structure of nucleic acids: A structure for deoxyribose nucleic acid. Nature. 1953; 171: 737–738. PMID: 13054692
3. Löwdin P-O. Proton tunneling in DNA and its biological implications. Rev Mod Phys. 1963; 35: 724–732.
4. Löwdin P-O. Quantum genetics and the aperiodic solid: Some aspects on the biological problems of heredity, mutations, aging, and tumors in view of the quantum theory of the DNA molecule. In: Löwdin P-O, editor. Advances in quantum chemistry. New York, USA, London, UK: Academic Press; 1966: 2. pp. 213–360.
5. Topal MD, Fresco JR. Complementary base pairing and the origin of substitution mutations. Nature. 1976; 263: 285–289. PMID: 958482
6. Brovarets' OO. Microstructural mechanisms of the origin of the spontaneous point mutations. DrSci Thesis, Taras Shevchenko National University of Kyiv, 2015.
7. Florian J, Hrouda V, Hobza P. Proton transfer in the adenine-thymine base pair. J Am Chem Soc. 1994; 116: 1457–1460.
8. Gorb L, Podolyan Y, Dziekonski P, Sokalski WA, Leszczynski J. Double-proton transfer in adenine −thymine and guanine−cytosine base pairs. A post-Hartree-Fock *ab initio* study. J Am Chem Soc. 2004; 126: 10119–10129. https://doi.org/10.1021/ja049155n PMID: 15303888
9. Bertran J, Blancafort L, Noguera M, Sodupe M. Proton transfer in DNA base pairs. In: Šponer J, Lankaš F, editors. Computational studies of RNA and DNA. Dordrecht: Springer; 2006. pp. 411–432.
10. Cerón-Carrasco JP, Requena A, Michaux C, Perpète EA, Jacquemin D. Effects of hydration on the proton transfer mechanism in the adenine-thymine base pair. J Phys Chem A. 2009; 113: 7892–7898. https://doi.org/10.1021/jp900782h PMID: 19569720
11. Cerón-Carrasco JP, Jacquemin D. Electric field induced DNA damage: an open door for selective mutations. Chem Commun. 2013; 49: 7578–7580.

12. Arabi AA, Matta CF. Effects of external electric fields on double proton transfer kinetics in the formic acid dimer. Phys Chem Chem Phys. 2011; 13: 13738–13748. https://doi.org/10.1039/c1cp20175a PMID: 21720646

13. Brovarets' OO, Zhurakivsky RO, Hovorun DM. Is there adequate ionization mechanism of the spontaneous transitions? Quantum-chemical investigation. Biopol Cell, 2010; 26: 398–405.

14. Maximoff SN, Kamerlin ShCL, Florián J. DNA Polymerase λ active site favors a mutagenic mispair between the enol form of deoxyguanosine triphosphate substrate and the keto form of thymidine template: a free energy perturbation study. J Phys Chem B. 2017; 121: 7813–7822. https://doi.org/10.1021/acs.jpcb.7b04874 PMID: 28732447

15. Brovarets' OO, Kolomiets' IM, Hovorun DM. Elementary molecular mechanisms of the spontaneous point mutations in DNA: A novel quantum-chemical insight into the classical understanding. In: Tada Tomofumi, editor. Quantum chemistry—molecules for innovations. InTech Open Access; 2012.

16. Brovarets' OO, Hovorun DM. Can tautomerisation of the A·T Watson-Crick base pair via double proton transfer provoke point mutations during DNA replication? A comprehensive QM and QTAIM analysis. J Biomol Struct Dynam. 2014; 32: 127–154.

17. Brovarets' OO, Hovorun DM. Why the tautomerization of the G·C Watson–Crick base pair via the DPT does not cause point mutations during DNA replication? QM and QTAIM comprehensive analysis. J Biomol Struct Dynam. 2014; 32: 1474–1499.

18. Brovarets' OO, Hovorun DM. Proton tunneling in the A·T Watson-Crick DNA base pair: myth or reality? J Biomol Struct Dynam. 2015; 12: 2716–2720.

19. Brovarets' OO, Hovorun DM. New structural hypostases of the A·T and G·C Watson-Crick DNA base pairs caused by their mutagenic tautomerisation in a wobble manner: a QM/QTAIM prediction. RSC Adv. 2015; 5: 99594–99605.

20. Brovarets' OO, Tsiupa KS, Hovorun DM. The A·T(rWC)/A·T(H)/A·T(rH) ↔ A·T*(rwWC)/A·T*(wH)/A·T*(rwH) mutagenic tautomerization via sequential proton transfer: a QM/QTAIM study. RSC Adv. 2018; 8: 13433–13445.

21. Brovarets' OO, Hovorun DM. Wobble↔Watson-Crick tautomeric transitions in the homo-purine DNA mismatches: a key to the intimate mechanisms of the spontaneous transversions. J Biomol Struct Dynam. 2015; 33: 2710–2715.

22. Brovarets' OO, Hovorun DM. Novel physico-chemical mechanism of the mutagenic tautomerisation of the Watson–Crick-like A·G and C·T DNA base mispairs: a quantum-chemical picture. RSC Adv. 2015; 5: 66318–66333.

23. Brovarets' OO, Hovorun DM. A novel conception for spontaneous transversions caused by homo-pyrimidine DNA mismatches: a QM/QTAIM highlight. Phys Chem Chem Phys. 2015; 17: 21381–21388. https://doi.org/10.1039/c5cp03211c PMID: 26219928

24. Brovarets' OO, Hovorun DM. Physicochemical mechanism of the wobble DNA base pairs Gua·Thy and Ade·Cyt transition into the mismatched base pairs Gua*·Thy and Ade·Cyt* formed by the mutagenic tautomers. Ukr Bioorg Acta. 2009; 8: 12–18.

25. Brovarets' OO, Hovorun DM. Tautomeric transition between wobble A·C DNA base mispair and Watson-Crick-like A·C* mismatch: miscrostructural mechanism and biological significance. Phys Chem Chem Phys. 2015; 17: 15103–15110. https://doi.org/10.1039/c5cp01568e PMID: 25994250

26. Brovarets' OO, Hovorun DM. By how many tautomerisation routes the Watson-Crick-like A·C* DNA base mispair is linked with the wobble mismatches? A QM/QTAIM vision from a biological point of view. Struct Chem. 2016; 27: 119–131.

27. Brovarets' OO, Hovorun DM. How many tautomerisation pathways connect Watson-Crick-like G*·T DNA base mispair and wobble mismatches? J Biomol Struct Dynam. 2015; 33: 2297–2315.

28. Nedderman AN, Stone MJ, Lin PKT, Brown DM, Williams DH. Base pairing of cytosine analogues with adenine and guanine in oligonucleotide duplexes: evidence for exchange between Watson-Crick and wobble base pairs using ^{1}H NMR spectroscopy. J Chem Soc Chem Commun. 1991: 1357–1359.

29. Nedderman AN, Stone MJ, Williams DH, Lin PKY, Brown DM. Molecular basis for methoxyamine-initiated mutagenesis: ^{1}H nuclear magnetic resonance studies of oligonucleotide duplexes containing base-modified cytosine residues. J Mol Biol. 1993; 230: 1068–1076. https://doi.org/10.1006/jmbi.1993.1219 PMID: 8478918

30. Kimsey IJ, Petzold K, Sathyamoorthy B, Stein ZW, Al-Hashimi HM. Visualizing transient Watson-Crick-like mispairs in DNA and RNA duplexes. Nature. 2015; 519: 315–320. https://doi.org/10.1038/nature14227 PMID: 25762137

31. Szymanski ES, Kimsey IJ, Al-Hashimi HM. Direct NMR evidence that transient tautomeric and anionic states in dG·dT form Watson-Crick-like base pairs. J Am Chem Soc. 2017; 139: 4326–4329. https://doi.org/10.1021/jacs.7b01156 PMID: 28290687

32. Acosta-Reyes FJ, Alechaga E, Subirana JA, Campos JL. Structure of the DNA duplex d(ATTAAT)2 with Hoogsteen hydrogen bonds. PLoS One. 2015; 10: e0120241. https://doi.org/10.1371/journal.pone.0120241 PMID: 25781995

33. Müller J. Metal-mediated base pairs in parallel-stranded DNA. Beilstein J Org Chem. 2017; 13: 2671–2681. https://doi.org/10.3762/bjoc.13.265 PMID: 29564004

34. Zhou H. Occurrence and function of Hoogsteen base pairs in nucleic acids. PhD Thesis, Duke University, 2016. https://dukespace.lib.duke.edu/dspace/handle/10161/12892

35. Tchurikov NA, Chernov BK, Golova YB, Nechipurenko YD. Parallel DNA: Generation of a duplex between two Drosophila sequences *in vitro*. FEBS Lett. 1989; 257: 415–418. PMID: 2479581

36. Cubero E, Luque FJ, Orozco M. Theoretical studies of d(A:T)-based parallel-stranded DNA duplexes. J Am Chem Soc. 2001; 123: 12018–12025. PMID: 11724610

37. Parvathy VR, Bhaumik SR, Chary KV, Govil G, Liu K, Howard FB, Miles HT. NMR structure of a parallel-stranded DNA duplex at atomic resolution. Nucleic Acids Res. 2002; 30: 1500–1511. PMID: 11917010

38. Poltev VI, Anisimov VM, Sanchez C, Deriabina A, Gonzalez E, Garcia D, Rivas N, Polteva NA. Analysis of the conformational features of Watson–Crick duplex fragments by molecular mechanics and quantum mechanics methods. Biophysics 2016; 61: 217–226.

39. Ye MY, Zhu RT, Li X, Zhou XS, Yin ZZ, Li Q, Shao Y. Adaptively recognizing parallel-stranded duplex structure for fluorescent DNA polarity analysis. Anal Chem. 2017; 89: 8604–8608. https://doi.org/10.1021/acs.analchem.7b02467 PMID: 28812355

40. Szabat M, Kierzek R. Parallel-stranded DNA and RNA duplexes: structural features and potential applications. FEBS J. 2017; 284: 3986–3998. https://doi.org/10.1111/febs.14187 PMID: 28771935

41. Brovarets' OO. Under what conditions does G·C Watson-Crick DNA base pair acquire all four configurations characteristic for A·T Watson-Crick DNA base pair? Ukr Biochem J. 2013; 85: 98–103.

42. Brovarets' OO. Structural and energetic properties of the four configurations of the A·T and G·C DNA base pairs. Ukr Biochem J. 2013; 85: 104–110.

43. Hoogsteen K. The crystal and molecular structure of a hydrogenbonded complex between 1-methylthymine and 9-methyladenine. Acta Cryst. 1963; 16: 907–916.

44. Abrescia NG, Thompson A, Huynh-Dinh T, Subirana JA. Crystal structure of an antiparallel DNA fragment with Hoogsteen base pairing. Proc Natl Acad Sci USA. 2002; 99: 2806–2811. https://doi.org/10.1073/pnas.052675499 PMID: 11880632

45. Abrescia NG, Gonzalez C, Gouyette C, Subirana JA. X-ray and NMR studies of the DNA oligomer d(ATATAT): Hoogsteen base pairing in duplex DNA. Biochemistry 2004; 43: 4092–4100. https://doi.org/10.1021/bi0355140 PMID: 15065851

46. Pous J, Urpi L, Subirana JA, Gouyette C, Navaza J, Campos JL. Stabilization by extra-helical thymines of a DNA duplex with Hoogsteen base pairs. J Am Chem Soc. 2008; 130: 6755–6760. https://doi.org/10.1021/ja078022+ PMID: 18447354

47. Campos L, Valls N, Urpí L, Gouyette C, Sanmartín T, Richter M, Alechaga E, Santaolalla A, Baldini R, Creixell M, Ciurans R, Skokan P, Pous J, Subirana JA. Overview of the structure of all AT oligonucleotides: organization in helices and packing interactions. Biophys J. 2006; 91: 892–903. https://doi.org/10.1529/biophysj.106.084210 PMID: 16698788

48. Nikolova EN, Zhou H, Gottardo FL, Alvey HS, Kimsey IJ, Al-Hashimi HM. A historical account of Hoogsteen base-pairs in duplex DNA. Biopolymers 2014; 99: 955–968.

49. Alvey HS, Gottardo FL, Nikolova EN, Al-Hashimi HM. Widespread transient Hoogsteen base-pairs in canonical duplex DNA with variable energetics. Nature Comm. 2014; 5: 4786–4794.

50. Frisch MJ, Trucks GW, Schlegel HB, Scuseria GE, Robb MA, Cheeseman JR, et al. GAUSSIAN 09 (Revision B.01). Wallingford CT: Gaussian Inc; 2010.

51. Tirado-Rives J, Jorgensen WL. Performance of B3LYP Density Functional Methods for a large set of organic molecules. J Chem Theory Comput. 2008; 4: 297–306. https://doi.org/10.1021/ct700248k PMID: 26620661

52. Parr RG, Yang W. Density-functional theory of atoms and molecules. Oxford: Oxford University Press; 1989.

53. Lee C, Yang W, Parr RG. Development of the Colle-Salvetti correlation-energy formula into a functional of the electron density. Phys Rev B. 1988; 37: 785–789.

54. Hariharan PC, Pople JA. The influence of polarization functions on molecular orbital hydrogenation energies. Theor Chim Acta. 1973; 28: 213−222.

55. Krishnan R, Binkley JS, Seeger R, Pople JA. Self-consistent molecular orbital methods. XX. A basis set for correlated wave functions. J Chem Phys. 1980; 72: 650−654.

56. Matta CF. How dependent are molecular and atomic properties on the electronic structure method? Comparison of Hartree-Fock, DFT, and MP2 on a biologically relevant set of molecules. J Comput Chem. 2010; 31: 1297–1311. https://doi.org/10.1002/jcc.21417 PMID: 19882732

57. Gatti C, Macetti G, Boyd RJ, Matta CF. An electron density source-function study of DNA base pairs in their neutral and ionized ground states. J Comput Chem. 2018; 39: 1112–1128. https://doi.org/10.1002/jcc.25222 PMID: 29681131

58. Arabi A, Matta CF Adenine–thymine tautomerization under the influence of strong homogeneous electric fields, Phys Chem Chem Phys. 2018; 20: 12406–12412. https://doi.org/10.1039/c8cp01122b PMID: 29693088

59. Brovarets' OO, Hovorun DM. Quantum-chemical investigation of tautomerization ways of Watson-Crick DNA base pair guanine-cytosine. Ukr Biochem J. 2010; 82: 55–60.

60. Brovarets' OO, Hovorun DM. Quantum-chemical investigation of the elementary molecular mechanisms of pyrimidine·purine transversions. Ukr Biochem J. 2010; 82: 57–67.

61. Brovarets' OO, Zhurakivsky RO, Hovorun DM. The physico-chemical "anatomy" of the tautomerisation through the DPT of the biologically important pairs of hypoxanthine with DNA bases: QM and QTAIM perspectives. J. Mol. Model. 2013: 19: 4119–4137. https://doi.org/10.1007/s00894-012-1720-9 PMID: 23292249

62. Brovarets' OO, Zhurakivsky RO, Hovorun DM. The physico-chemical mechanism of the tautomerisation *via* the DPT of the long Hyp*·Hyp Watson-Crick base pair containing rare tautomer: a QM and QTAIM detailed look. Chem Phys Lett. 2013; 578: 126–132.

63. Brovarets' OO, Hovorun DM. How the long G·G* Watson-Crick DNA base mispair comprising keto and enol tautomers of the guanine tautomerises? The results of the QM/QTAIM investigation. Phys Chem Chem Phys. 2014; 6: 15886–15899.

64. Brovarets' OO, Zhurakivsky RO, Hovorun DM. DPT tautomerisation of the wobble guanine·thymine DNA base mispair is not mutagenic: QM and QTAIM arguments. J Biomol Struct Dynam. 2015; 33: 674–689.

65. Palafox MA. Molecular structure differences between the antiviral nucleoside analogue 5-iodo-2'-deoxyuridine and the natural nucleoside 2'-deoxythymidine using MP2 and DFT methods: conformational analysis, crystal simulations, DNA pairs and possible behavior. J Biomol Struct Dynam. 2014; 32: 831–851.

66. El-Sayed AA, Tamara Molina A. Alvarez-Ros MC, Palafox MA. Conformational analysis of the anti-HIV Nikavir prodrug: comparisons with AZT and thymidine, and establishment of structure-activity relationships/tendencies in other 60-derivatives. J Biomol Struct Dynam. 2015; 33: 723–748.

67. Hratchian HP, Schlegel HB. Finding minima, transition states, and following reaction pathways on *ab initio* potential energy surfaces. In: Dykstra CE, Frenking G, Kim KS, Scuseria G., editor. Theory and applications of computational chemistry: The first 40 years. Amsterdam: Elsevier; 2005. pp. 195–249.

68. Yepes D, Murray JS, Politzer P, Jaque P. The reaction force constant: an indicator of the synchronicity in double proton transfer reactions. Phys Chem Chem Phys. 2012; 14: 11125–11134. https://doi.org/10.1039/c2cp41064h PMID: 22782086

69. Inostroza-Rivera R, Yahia-Ouahmed M, Tognetti V, Joubert L, Herrera B, Toro-Labbé A. Atomic decomposition of conceptual DFT descriptors: application to proton transfer reactions. Phys Chem Chem Phys. 2015; 17: 17797–17808. https://doi.org/10.1039/c5cp01515d PMID: 26089126

70. Peng C, Ayala PY, Schlegel HB, Frisch MJ. Using redundant internal coordinates to optimize equilibrium geometries and transition states. J Comput Chem. 1996; 17: 49–56.

71. Atkins PW. Physical chemistry. Oxford: Oxford University Press; 1998.

72. Frisch MJ, Head-Gordon M, Pople JA. Semi-direct algorithms for the MP2 energy and gradient. Chem Phys Lett. 1990; 166: 281–289.

73. Kendall RA, Dunning TH Jr, Harrison RJ. Electron affinities of the first-row atoms revisited. Systematic basis sets and wave functions. J Chem Phys. 1992; 96: 6796−6806.

74. Brovarets' OO, Pérez-Sánchez HE, Hovorun DM. Structural grounds for the 2-aminopurine mutagenicity: A novel insight into the old problem of the replication errors. RSC Adv. 2016; 6: 99546–99557.

75. Brovarets' OO, Pérez-Sánchez HE. Whether 2-aminopurine induces incorporation errors at the DNA replication? A quantum-mechanical answer on the actual biological issue. J Biomol Struct Dynam. 2017; 35: 3398–3411.

76. Brovarets' OO, Pérez-Sánchez HE. Whether the amino-imino tautomerism of 2-aminopurine is involved into its mutagenicity? Results of a thorough QM investigation. RSC Adv. 2016; 110: 108255–108264.

77. Brovarets' OO, Voiteshenko IS, Pérez-Sánchez HE, Hovorun DM. A QM/QTAIM research under the magnifying glass of the DPT tautomerisation of the wobble mispairs involving 2-aminopurine. New J Chem. 2017; 41: 7232–7243.

78. Brovarets' OO, Voiteshenko IS, Hovorun DM. Physico-chemical profiles of the wobble↔Watson-Crick G*·2AP(w)↔G·2AP(WC) and A·2AP(w)↔A*·2AP(WC) tautomerisations: A QM/QTAIM comprehensive survey. Phys Chem Chem Phys. 2018; 20: 623–636.

79. Brovarets' OO, Voiteshenko I, Pérez-Sánchez HE, Hovorun DM. A QM/QTAIM detailed look at the Watson-Crick↔wobble tautomeric transformations of the 2-aminopurine·pyrimidine mispairs. J Biomol Struct Dynam. 2018; 36: 1649–1665.

80. Jurecka P, Sponer J, Cerný J, Hobza P. Benchmark database of accurate (MP2 and CCSD(T) complete basis set limit) interaction energies of small model complexes, DNA base pairs, and amino acid pairs. Phys Chem Chem Phys. 2006; 8:1985–1993. https://doi.org/10.1039/b600027d PMID: 16633685

81. Jurečka P, Šponer J, Černý J, Hobza P Benchmark database of accurate (MP2 and CCSD(T) complete basis set limit) interaction energies of small model complexes, DNA base pairs, and amino acid pairs. Phys Chem Chem Phys. 2006; 8:1985–1993. https://doi.org/10.1039/b600027d PMID: 16633685

82. Zoete V, Meuwly M. Double proton transfer in the isolated and DNA-embedded guanine-cytosine base pair. J Chem Phys. 2004; 121: 4377–4388. https://doi.org/10.1063/1.1774152 PMID: 15332989

83. Negi I, Kathuria P, Sharma P, Wetmore SD. How do hydrophobic nucleobases differ from natural DNA nucleobases? Comparison of structural features and duplex properties from QM calculations and MD simulations. Phys Chem Chem Phys. 2017; 19: 16365–16374. https://doi.org/10.1039/c7cp02576a PMID: 28657627

84. Felske LR, Lenz SAP, Wetmore SD. Quantum chemical studies of the structure and stability of N-methylated DNA nucleobase dimers: insights into the mutagenic base pairing of damaged DNA. J Phys Chem A. 2018; 122: 410–419. https://doi.org/10.1021/acs.jpca.7b10485 PMID: 29189004

85. Brovarets' OO, Tsiupa KS, Hovorun DM. Surprising conformers of the biologically important A·T DNA base pairs: QM/QTAIM proofs. Front Chem. 2018; 6: 8; https://doi.org/10.3389/fchem.2018.00008 PMID: 29536003

86. Boys SF, Bernardi F. The calculation of small molecular interactions by the differences of separate total energies. Some procedures with reduced errors. Mol Phys. 1970; 19: 553–566.

87. Gutowski M, Van Lenthe JH, Verbeek J, Van Duijneveldt FB, Caahalasinski G. The basis set superposition error in correlated electronic structure calculations. Chem Phys Lett. 1986; 124: 370–375.

88. Sordo JA, Chin S, Sordo TL. On the counterpoise correction for the basis set superposition error in large systems. Theor Chim Acta. 1988; 74: 101–110.

89. Sordo JA. On the use of the Boys–Bernardi function counterpoise procedure to correct barrier heights for basis set superposition error. J Mol Struct. 2001; 537: 245–251.

90. Šponer J, Jurecka P, Hobza P. Accurate interaction energies of hydrogen-bonded nucleic acid base pairs. J Am Chem Soc. 2004; 126: 10142–10051. https://doi.org/10.1021/ja048436s PMID: 15303890

91. Bader RFW. Atoms in molecules: A quantum theory. Oxford: Oxford University Press; 1990.

92. Matta CF, Hernández-Trujillo J. Bonding in polycyclic aromatic hydrocarbons in terms of the electron density and of electron delocalization. J Phys Chem A. 2003; 107: 7496–7504.

93. Matta CF, Castillo N, Boyd RJ. Atomic contributions to bond dissociation energies in aliphatic hydrocarbons. J Chem Phys. 2006; 125: 204103. https://doi.org/10.1063/1.2378720 PMID: 17144686

94. Cukrowski I, Matta CF. Hydrogen–hydrogen bonding: A stabilizing interaction in strained chelating rings of metal complexes in aqueous phase. Chem Phys Lett. 2010; 499: 66–69.

95. Matta CF. Modeling biophysical and biological properties from the characteristics of the molecular electron density, electron localization and delocalization matrices, and the electrostatic potential. J Comput Chem. 2014; 35: 1165–1198. https://doi.org/10.1002/jcc.23608 PMID: 24777743

96. Lecomte C, Espinosa E, Matta CF. On atom–atom 'short contact' bonding interactions in crystals, IUCrJ. 2015; 2: 161–163. https://doi.org/10.1107/S2052252515002067 PMID: 25866651

97. Keith TA. AIMAll (Version 10.07.01); 2010. Retrieved from aim.tkgristmill.com.

98. Matta CF, Castillo N, Boyd RJ. Extended weak bonding interactions in DNA: π-stacking (base-base), base-backbone, and backbone-backbone interactions. J Phys Chem B. 2006; 110: 563–578. https://doi.org/10.1021/jp054986g PMID: 16471569

99. Brovarets' OO, Zhurakivsky RO, Hovorun DM. Is the DPT tautomerisation of the long A·G Watson-Crick DNA base mispair a source of the adenine and guanine mutagenic tautomers? A QM and

QTAIM response to the biologically important question. J Comput Chem. 2014; 35: 451–466. https://doi.org/10.1002/jcc.23515 PMID: 24382756

100. Brovarets' OO, Hovorun DM. DPT tautomerisation of the G·A_{syn} and A*·G*$_{syn}$ DNA mismatches: A QM/QTAIM combined atomistic investigation. Phys Chem Chem Phys. 2014; 16: 9074–9085. https://doi.org/10.1039/c4cp00488d PMID: 24695821

101. Matta CF, Boyd RJ. The Quantum Theory of Atoms in Molecules: from solid state to DNA and drug design. Weinheim: Wiley-VCH Verlag GmbH & Co. KGaA; 2007.

102. Brovarets' OO, Zhurakivsky RO, Hovorun DM. Structural, energetic and tautomeric properties of the T·T*/T*·T DNA mismatch involving mutagenic tautomer of thymine: a QM and QTAIM insight. Chem Phys Lett. 2014; 592: 247–255.

103. Espinosa E, Molins E, Lecomte C. Hydrogen bond strengths revealed by topological analyses of experimentally observed electron densities. Chem Phys Lett. 1998; 285: 170–173.

104. Mata I, Alkorta I, Espinosa E, Molins E. Relationships between interaction energy, intermolecular distance and electron density properties in hydrogen bonded complexes under external electric fields. Chem Phys Lett. 2011; 507: 185–189.

105. Iogansen AV. Direct proportionality of the hydrogen bonding energy and the intensification of the stretching v(XH) vibration in infrared spectra. Spectrochim Acta Part A: Mol Biomol Spectrosc. 1999; 55: 1585–1612.

106. Brovarets' OO, Hovorun DM. The nature of the transition mismatches with Watson-Crick architecture: the G*·T or G·T* DNA base mispair or both? A QM/QTAIM perspective for the biological problem. J Biomol Struct Dynam. 2015; 33: 925–945.

107. Brovarets' OO, Hovorun DM. The physicochemical essence of the purine·pyrimidine transition mismatches with Watson-Crick geometry in DNA: A·C* *versa* A*·C. A QM and QTAIM atomistic understanding. J Biomol Struct Dynam. 2015; 33: 28–55.

108. Saenger W. Principles of nucleic acid structure. New York: Springer; 1984.

109. Nikolaienko TY, Bulavin LA, Hovorun DM. Bridging QTAIM with vibrational spectroscopy: The energy of intramolecular hydrogen bonds in DNA-related biomolecules. Phys Chem Chem Phys. 2012; 14: 7441–7447. https://doi.org/10.1039/c2cp40176b PMID: 22514024

110. Brovarets' OO, Yurenko YP, Hovorun D M. Intermolecular CH···O/N H-bonds in the biologically important pairs of natural nucleobases: A thorough quantum-chemical study. J Biomol Struct Dynam. 2014; 32: 993–1022.

111. Brovarets' OO, Yurenko YP, Hovorun DM. The significant role of the intermolecular CH···O/N hydrogen bonds in governing the biologically important pairs of the DNA and RNA modified bases: a comprehensive theoretical investigation. J Biomol Struct Dynam. 2015: 33: 1624–1652.

112. Brovarets' OO, Hovorun DM. Does the G·G*$_{syn}$ DNA mismatch containing canonical and rare tautomers of the guanine tautomerise through the DPT? A QM/QTAIM microstructural study. Mol Phys. 2014; 112: 3033–3046.

113. Brovarets' OO, Hovorun DM. Atomistic mechanisms of the double proton transfer in the H-bonded nucleobase pairs: QM/QTAIM computational lessons. J Biomol Struct Dyn. 2018 (in press).

114. Samijlenko SP, Krechkivska OM, Kosach DA, Hovorun DM. Transitions to high tautomeric states can be induced in adenine by interactions with carboxylate and sodium ions: DFT calculation data. J Mol Struct. 2004; 708: 97–104.

115. Drake JW, Charlesworth B, Charlesworth D, Crow JF. Rates of spontaneous mutation. Genetics 1998; 148: 1667–1686. PMID: 9560386

116. Lynch M. Rate, molecular spectrum, and consequences of human mutation. Proc Natl Acad Sci USA. 2010; 107: 961–968. https://doi.org/10.1073/pnas.0912629107 PMID: 20080596

117. Fijalkowska IJ, Schaaper RM, Jonczyk P. DNA replication fidelity in *Escherichia coli*: a multi-DNA polymerase affair. FEMS Microbiol Rev. 2012; 36: 1105–1121. https://doi.org/10.1111/j.1574-6976.2012.00338.x PMID: 22404288

118. Govorun DM, Danchuk VD, Mishchuk YaR, Kondratyuk IV, Radomsky NF, Zheltovsky NV. AM1 calculation of the nucleic acid bases structure and vibrational spectra. J. Mol. Struct. 1992; 267: 99–103.

119. Nikolaienko TY, Bulavin LA, Hovorun DM. How flexible are DNA constituents? The quantum-mechanical study. J Biomol Struct Dynam. 2011; 29: 563–575.

120. Hovorun DM, Gorb L, Leszczynski J. From the nonplanarity of the amino group to the structural nonrigidity of the molecule: a post-Hartree-Fock *ab initio* study of 2-aminoimidazole. Int J Quantum Chem. 1999; 75: 245–253.

121. Salam T, Devi SP, Lyngdoh RHD. Molecular criteria for mutagenesis by DNA methylation: some computational elucidations. Mutat Res Fund Mol Mech Mutagen. 2018; 807: 10–20.

122. Lyngdoh RHD. Mutagenic role of Watson–Crick protons in alkylated DNA bases: A theoretical study. J Biosciences 1994; 19: 131–143.

123. Venkateswarlu D, Lyngdoh RHD. Mutagenic significance of proton acidities in methylated guanine and thymine bases and deoxynucleosides: A theoretical study. J Mol Struct Theochem. 1997; 393: 151–161.

124. Venkateswarlu D, Lyngdoh RHD. Structural, steric and energetic requirements for induction of base substitutional mutations by methylated guanines and thymines. J Chem Soc Perkin Trans. 1995; 2: 839–846.